Hydrogen-Bonding Interaction in Molecular Complexes and Clusters of Aerosol Nucleation Precursors

Jun Zhao,[†] Alexei Khalizov, and Renyi Zhang*

Department of Atmospheric Sciences and Department of Chemistry, Texas A&M University, College Station, Texas 77843

Robert McGraw

Atmospheric Sciences Division, Brookhaven National Laboratory, P.O. Box 5000, Upton, New York 11973

Received: July 28, 2008; Revised Manuscript Received: October 16, 2008

Complexes and clusters bridge the gap between molecular and macroscopic levels by linking individual gaseous molecules to newly formed nanoparticles but the driving forces and mechanism for the formation of complexes and clusters in the atmosphere are not well understood. We have performed ab initio and density functional quantum chemical calculations to elucidate the role of organic acids in the formation of complexes with common atmospheric nucleating precursors such as sulfuric acid, water, and ammonia. A central feature of the complexes is the presence of two hydrogen bonds. Organic acid−sulfuric acid complexes show one strong and one medium-strength hydrogen bond whereas the corresponding hydrogen bonds in organic acid−ammonia complexes are characterized as medium-strength and weak. The formation of strong hydrogen bonds in organic acid−sulfuric acid complexes is explained by the well-established resonance-assisted hydrogen bonding theory. Organic acid−sulfuric acid and organic acid−organic acid complexes possess the largest binding energies among the homomolecular and heteromolecular dimers, about 18 kcal mol^{-1} from the composite theoretical methods. Topological analysis employing quantum theory of atoms in molecules (QTAIM) shows that the charge density and the Laplacian at bond critical points (BCPs) of the hydrogen bonds of the organic acid−sulfuric acid complex (e.g., benzoic acid−sulfuric acid and *cis*-pinonic acid−sulfuric acid) are 0.07 and 0.16 au, respectively, which falls in or exceeds the range of one strong and one medium-strength hydrogen bonding criteria.

1. Introduction

New particle formation involving sulfuric acid as a principal atmospheric nucleating agent represents an important contributor to nucleation mode aerosols.[1] Field measurements have consistently shown that sulfuric acid, while participating in nucleation, accounts for only a portion of the particle growth during the nucleation events in certain locations,[2,3] revealing that atmospheric new particles are essentially multicomponent in their chemical makeup. Other likely nucleating precursors include ubiquitous species like NH_3 and organic compounds. Experimental studies show that the binary $H_2SO_4-H_2O$ nucleation rates increase by up to several hundred fold in the presence of ppb-to-ppm (parts per billion to parts per million) levels of NH_3.[4,5] Classical and kinetic nucleation models predict even higher enhancement of the nucleation rates (up to 30 orders of magnitude) in the presence of ppt (parts per trillion) level of NH_3.[6−10] Field measurements have shown that atmospheric aerosol particles contain a substantial fraction of organic compounds.[1] Recent laboratory experiments have revealed that new particle formation in the binary sulfuric acid−water system is considerably enhanced in the presence of sub-ppb levels of aromatic acids (e.g., benzoic acid, *m*-toluic acid, *p*-toluic acid).[11]

Although atmospheric aerosol nucleation has received close attention over decades and continuous progress has been made toward understanding of the nucleation mechanism, new particle formation at a fundamental microscopic molecular level is still poorly understood. It is commonly recognized that molecular complexes and prenucleation clusters are at the initial stage of new particle formation. The molecular complexes and small clusters (usually smaller than 1 nm) containing up to several tens of molecules bridge the gap between individual molecules and newly nucleated particles (e.g., larger than 3 nm) and play a vital role in the atmospheric new particle formation process. Knowledge of the thermodynamic properties of these complexes and clusters is limited and the kinetics and dynamics of molecular processes for formation of molecular aggregates remain largely unclear, hindering efforts to quantitatively predict atmospheric nucleation rates.

The driving forces for the formation of atmospheric molecular complexes are hydrogen-bonding interactions, whose strength determines the thermodynamic stability of these complexes. Atmospherically relevant hydrogen-bonding complexes have been the subject of numerous theoretical studies in recent years. The complexes and clusters of sulfuric acid with other species (e.g., water, ammonia, and organics) are formed via hydrogen bonds of intermediate strength. Currently, the microscopic mechanism for atmospheric nucleation of the sulfuric acid−water system is not known, but in general hydrogen-bonding interaction represents the first step in this process, which determines the growth of clusters by condensation of sulfuric acid and other trace species. Due to the large affinity for water, gaseous sulfuric acid exists in hydrate form.[12,13] Previous quantum chemical

* Corresponding author. Fax: +979-862-4466. E-mail: zhang@ariel.met.tamu.edu.

[†] Present address: National Center for Atmospheric Research, Atmospheric Chemistry Division, Boulder, CO 80301.

10.1021/jp806693r CCC: $40.75
Published on Web 01/05/2009

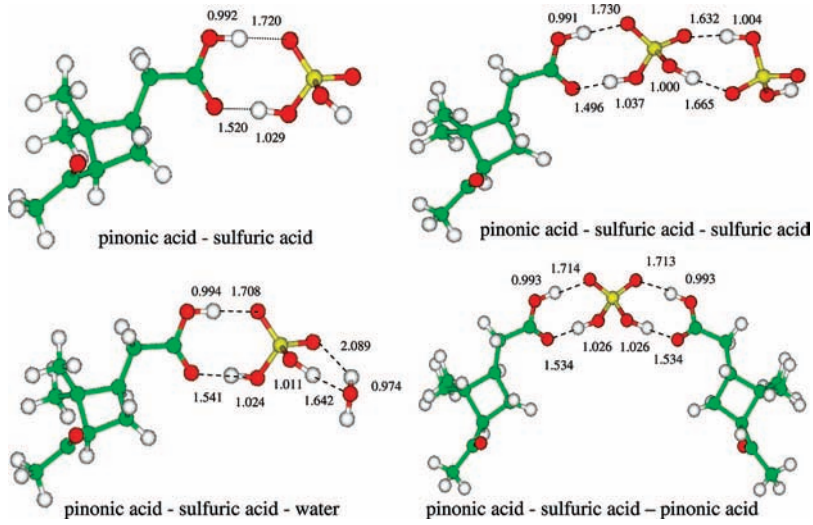

Figure 1. The optimized geometries of the complexes of sulfuric acid, *cis*-pinonic acid, and water at B3LYP/6-31G(d,p) level.

calculations focused on sulfuric acid hydrates $(H_2SO_4)_x(H_2O)_y$ ($x = 1-3$, $y = 0-9$) or sulfuric acid−ammonia complex and its hydrate clusters $(H_2SO_4)_x(H_2O)_y(NH_3)_z$ ($x = 1-2$, $y = 0-5$, $z = 1$).[14−25] Deprotonation of sulfuric acid and formation of ions have been shown to occur only in larger hydrated clusters, but there was little agreement regarding the role of ammonia in the stabilization of clusters.

From the microscopic molecular point of view, how organic compounds participate in the nucleation process remains an open question. Stable carboxylic acid dimers have been detected experimentally and studied theoretically.[26−30] It has been speculated that formation of stable dimers between carboxylic acids might be the first step in the new particle formation for the ozonolysis of pinenes.[31,32] Recent quantum chemical and modeling calculations indicate that formation of the unusually stable aromatic acid−sulfuric acid complex reduces the nucleation barrier and is responsible for the observed enhancement of the binary $H_2SO_4-H_2O$ nucleation in the presence of sub-ppb levels of organic acids.[11,33,34] Recently, Nadykto and Yu performed quantum chemical calculations to investigate the thermodynamic stability of the hydrogen-bonded complexes of small carboxylic acids (e.g., formic and acetic acid) with free and hydrated sulfuric acid, and with ammonia.[30] Their results indicated that both organic acids and ammonia may have efficiently stabilizing effects on the binary $H_2SO_4-H_2O$ clusters and the organic acids can interact actively with ammonia.

In this study we report a density functional and ab initio molecular orbital study of the molecular complexes of several atmospheric aerosol nucleating precursors (e.g., sulfuric acid, organic acids, water, and ammonia). Several organic acids are considered in this work, including *cis*-pinonic acid, which has been found as one of the most abundant low-volatile products from photooxidation of biogenic hydrocarbons (i.e., pinenes) emitted in significant quantities by vegetation.[35] Various ab initio and density functional quantum chemical calculations are employed to determine the geometries and energetics of the complexes and clusters. We also employed the quantum theory of atoms in molecules (QTAIM)[36] to elucidate the nature of the hydrogen bonds of these complexes and clusters and reveal their roles in new particle formation.

2. Theoretical Methods

Ab initio molecular orbital calculations were performed on an SGI Altix 3700 supercomputer with use of the Gaussian 03 software package.[37] All the species were treated with the restricted Hartree−Fock (RHF) formulation. Geometry optimization for complexes and their monomers was executed by using Becke's three-parameter hybrid funcional employing the LYP correction function (B3LYP) in conjunction with the split valence polarized basis set 6-31G(d,p). Harmonic vibrational frequency calculations were made by using B3LYP/6-31G(d,p) to confirm the energy minima for all the structures of the relevant complexes and monomers. For each stationary point, additional energy calculations were conducted by using B3LYP with 6-311++G(2d,2p) basis set and the basis set superposition error (BSSE) was evaluated by using the counterpoise correction method. The IR spectra for the complexes were obtained from the frequency calculations. The optimized structures were also employed in a series of single-point energy calculations by using coupled-cluster theory with single and double excitations including perturbative corrections for the triple excitations (CCSD(T)) with several larger Gaussian-type basis sets. Additional calculations were performed with use of composite methods G2(MP2, SVP)[38] and CCSD(T)+CF.[39] The basis set correction factor (CF) in CCSD(T)+CF was determined from the difference between MP2/6-311++G(d,p) and MP2/6−31G(d) total energies. The CCSD(T)+CF procedure has been developed and applied to study oxidation of several atmospheric hydrocarbons including isoprene, toluene, xylenes, and pinenes.[39−48]

The topological analysis was performed by using the quantum theory of atoms in molecules (QTAIM) of Bader[36] with the AIM2000 package[49−51] at the B3LYP/6-31G(d,p) level to investigate the nature of hydrogen-bonded complexes. We focused on the topological properties (e.g., charge density and its Laplacian, energy density) at hydrogen bond critical points (BCPs) to evaluate the strength of hydrogen-bonding interactions between sulfuric acid, ammonia, water and organic acids.

3. Results and Discussion

3.1. Geometrical Analysis. The geometries of H_2SO_4, H_2O, NH_3, and organic acids are optimized at the B3LYP/6-31G(d,p) level with use of the Gaussian 03 package.[37] The DFT-B3LYP has been proven to be an appropriate method for geometry optimization and frequency calculations, considering the trade-offs between the computational accuracy and efficiency for large organic acid molecules. The calculated structural parameters (e.g., bond length, bond angle) are in good agreement with the available experimental data (Supporting Information, Tables

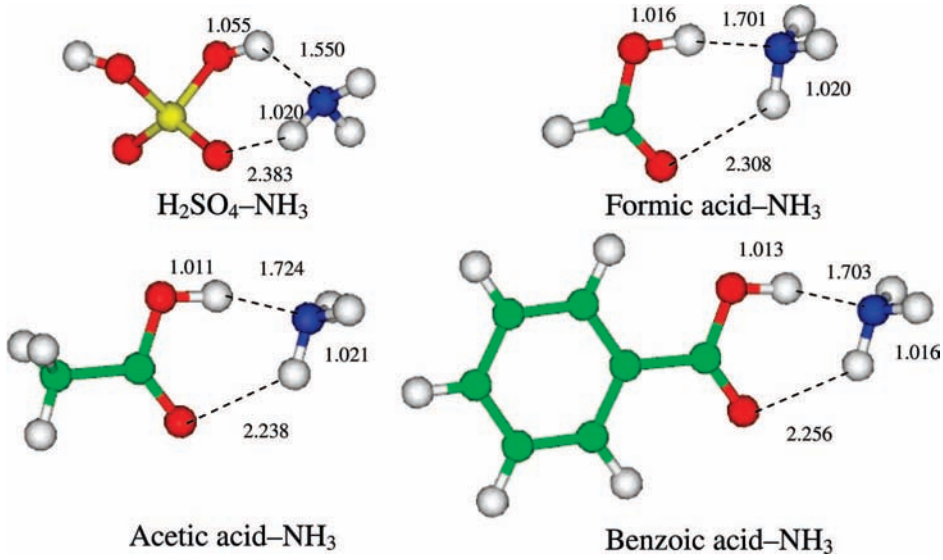

Figure 2. The optimized geometries of the complexes of sulfuric acid, organic acids, and ammonia at B3LYP/6-31G(d,p) level.

TABLE 1: Bond Lengths (in angstroms) and Bond Angles (in degrees) of the Hydrogen Bonds in the Complexes of Sulfuric Acid, Organic Acid, Ammonia, and Water[a]

complex[b]	r(H···O) or r(H···N)	α(O−H···O) or α(O−H···N)	r(H···O)	α(N−H···O) or α(O−H···O)
	hydrogen bond 1 (short)		hydrogen bond 2 (long)	
W-SA	1.627	164.7	2.094	130.2
BA-SA	1.503	177.13	1.705	178.5
PA-SA	1.520	177.1	1.720	178.0
SA-SA	1.653	175.6	1.653	175.6
BA-BA	1.616	178.7	1.616	178.7
PA-PA	1.640	179.1	1.640	179.1
SA-AM	1.550	171.9	2.383	117.8
FA-AM	1.701	165.8	2.308	123.7
AA-AM	1.724	165.3	2.238	126.5
BA-AM	1.703	166.5	2.256	125.1
PA-SA-W	1.541	177.5	1.708	178.1
PA-SA-SA	1.496	178.1	1.730	178.3
PA-SA-PA	1.534	178.1	1.714	178.3
	hydrogen bond 3 (short)		hydrogen bond 4 (long)	
PA-SA-W	1.592	163.2	2.089	131.5
PA-SA-SA	1.632	178.3	1.665	178.1
PA-SA-PA	1.535	178.1	1.713	178.2

[a] Bond lengths r(H···O) and angles α(O−H···O) are for structures optimized at the B3LYP/6-31G(d,p) level of theory. [b] W is water, SA is sulfuric acid, BA is benzoic acid, PA is *cis*-pinonic acid, AM is ammonia, FA is formic acid, and AA is acetic acid.

TABLE 2: Contact Distance d(O---O) (in angstroms) of the Hydrogen Bond (−O−H···O=) in the Organic Acid−Sulfuric Acid Complexes and Their Homomolecular Dimers[a]

complex	HB pair 1		HB pair 2	
BA-SA	2.536	2.698		
PA-SA	2.549	2.712		
PA-SA-W	2.565	2.702	2.625	2.831
PA-SA-SA	2.532	2.720	2.635	2.660
PA-SA-PA	2.560	2.707	2.561	2.706
SA-SA	2.652	2.652		
BA-BA	2.624	2.624		
PA-PA	2.646	2.646		

[a] Geometrical parameters are for structures optimized at the B3LYP/6-31G(d,p) level of theory.

S1and S2). The trans-conformation is adopted for sulfuric acid. The equilibrium structures of the optimized monomers are employed to construct the initial geometries of relevant complexes and search for the complex global minima. Several possible stable configurations of the complexes between sulfuric acid, organic acids, and ammonia are found, but only the most stable configuration is presented, which bears a hydrogen bond pair in the complex.

TABLE 3: The Calculated Shifts in Stretching Frequencies (in cm^{-1}) of Complexes Involving Sulfuric Acid, Benzoic Acid, *cis*-Pinonic Acid, Water, and Ammonia[a]

	assignment and shift				
complex	CO−H	C=O	SO−H	S=O	S−OH
SA-W			−756	−268	43
SA-SA			−509	−35	66
BA-SA	−421	−102	−1141	−298	81
BA-BA	−676	−60			
PA-SA	−391	−105	−1066	−297	59
PA-PA	−605	−62			
SA-AM			−1447	−68	68
FA-AM	−813	−47			
AA-AM	−747	−52			
BA-AM	−808	−43			

[a] Unscaled harmonic frequencies are calculated at the B3LYP/6-31G(d,p) level of theory.

Figures 1 and 2 depict the optimized geometries of the hydrogen-bonded complexes of *cis*-pinonic acid, sulfuric acid, and water and the complexes of sulfuric acid, several organic acids, and ammonia at the B3LYP/6-31G(d,p) level, respectively. The heteromolecular dimer complexes possess a hydrogen bond pair, which forms a six- or eight-membered cyclic ring. In all cases, the hydrogen bond donated by sulfuric acid is stronger than the bond accepted by sulfuric acid. The bonding in the trimer containing sulfuric acid, *cis*-pinonic acid, and/or water is characterized by the two pairs of hydrogen bonds connected through a molecule of sulfuric acid. The hydrogen bond (O−H···X) (X = O or N) is formed between the electron-deficient hydrogen and the high electron density oxygen or nitrogen. The length of the hydrogen bonds ranges from 1.496 to 1.724 Å for the stronger bonding and from 1.708 to 2.383 Å for the weaker bonding, as shown in Table 1. For sulfuric acid monohydrate, the hydrogen bond donated by sulfuric acid is significantly stronger than the accepted one, as indicated by the bond length (1.627 and 2.094 Å). These bond lengths are close to the values calculated at B3LYP/D95(d,p)[17] and PW91/TZP[24] levels of theory and in good agreement with the experimental

TABLE 4: Thermochemical Parameters for the Complex Formation Calculated at the B3LYP Level with Counterpoise Correction to the Energy[a]

	B3LYP/6-31G(d,p)					B3LYP/6-311++G(2d,2p)			
complex	E_{CP}	E_B	ΔH	ΔS	ΔG	E_{CP}	E_B	ΔH	ΔG
SA_W	4.13	10.16	−10.99	−31.92	−1.47	0.77	7.48	−8.31	1.21
SA_AM	2.64	15.45	−16.06	−30.24	−7.04	0.62	12.28	−12.88	−3.87
SA_SA	3.07	13.71	−13.78	−36.03	−3.04	1.16	11.68	−11.75	−1.01
BA_SA	3.54	16.29	−16.25	−37.03	−5.21	0.96	14.90	−14.87	−3.83
PA_SA	3.57	15.58	−15.56	−37.89	−4.26	0.96	14.26	−14.24	−2.94
BA_BA	3.90	15.62	−15.42	−37.70	−4.18	0.61	14.57	−14.37	−3.13
PA_PA	4.06	14.15	−14.01	−40.27	−2.00	0.61	13.37	−13.23	−1.22
FA_AM	2.82	10.26	−10.91	−30.59	−1.79	0.42	8.08	−8.72	0.40
AA_AM	2.90	9.51	−10.03	−30.75	−0.86	0.40	7.44	−7.97	1.20
BA_AM	2.79	10.00	−10.46	−30.78	−1.28	0.40	7.77	−8.23	0.95

[a] E_{CP} (kcal mol^{-1}) is the counterpoise correction; E_B (kcal mol^{-1}), ΔH (kcal mol^{-1}), ΔS (cal mol^{-1} K^{-1}), and ΔG (kcal mol^{-1}) are the changes in binding energy, enthalpy, entropy, and Gibbs free energy, respectively. Zero point energy, entropy, and thermal corrections to enthalpy and Gibbs free energy were calculated from vibrational analysis performed at the B3LYP/6-31G(d,p) level of theory (1 atm, 298 K).

data (1.645 and 2.05 Å) by Fiacco et al.[52] A similar characteristic feature is found in the sulfuric acid−ammonia complex; the O−H···N hydrogen bond (1.550 Å) is substantially shorter than the N−H···O hydrogen bond (2.383 Å), indicating sulfuric acid as the hydrogen donor and water and ammonia as the hydrogen acceptor in both sulfuric acid monohydrate and sulfuric acid−ammonia complexes.

The hydrogen bonds in the organic acid−sulfuric acid complexes are comparable in length, differing by ∼0.2 Å for the *cis*-pinonic acid−sulfuric acid and benzoic acid−sulfuric acid complexes. In the organic acid−sulfuric acid complexes there is one vacant electron-deficient hydrogen atom in the sulfuric acid moiety that allows further addition of water, sulfuric acid, or organic acid, resulting in the formation of a trimer with a hydrogen bond pair similar to the one mentioned above. The sulfuric acid molecule is located in the center of the trimer and shared by the two cyclic hydrogen-bonded rings. A pair of hydrogen bonds with equivalent strength are formed in the homomolecular dimer of sulfuric acid, benzoic acid, and *cis*-pinonic acid. In the organic acid−ammonia complexes, the hydrogen bond (1.70−1.72 Å) donated by sulfuric acid is weaker than the corresponding hydrogen bond in the sulfuric acid−ammonia complex whereas the accepted one is comparable to that in the sulfuric acid−ammonia complex (2.24 to 2.31 vs 2.38 Å). Hence, the interactions between organic acids and ammonia are likely weaker than those between sulfuric acid and ammonia.

The interactions between organic acids and sulfuric acid involve a category of homonuclear hydrogen bonds (−O−H···O═) where two oxygen atoms are interconnected by a system of π-conjugated double bonds, the so-called resonance-assisted hydrogen bonding (RAHB).[53−59] The contact distance d(O---O) between the two oxygen atoms in the hydrogen bond (−O−H···O═) has been employed as an indicator of the hydrogen bond strength.[56] This distance is classified as very strong for d(O---O) < 2.5 Å, strong for 2.5 < d(O---O) <2.65 Å, medium for 2.65 < d(O---O) < 2.80 Å, and weak for d(O---O) > 2.8 Å. As shown in Table 2, all of the stronger hydrogen bonds of the pairs in the dimer and trimer fall into the strong hydrogen bond category with d(O---O) of 2.53−2.63 Å, while all the weaker hydrogen bonds in these complexes belong to the medium-strength hydrogen bond with d(O---O) of 2.66−2.72 Å. Another characteristic feature for this category of hydrogen bonding is the bond angles (−O−H···O═) close to 180° and the cyclic ring connected by the hydrogen bond pair forming a plane and serving as a strong connection between two moieties. These results indicate that the molecular interaction between organic acid and sulfuric acid is via the formation of a hydrogen bond pair with one strong and one medium-strength hydrogen bond. The heteronuclear hydrogen bonds (O−H···N and N−H···O) in the complexes of organic acids and ammonia are weaker than those in organic acid−sulfuric acid complexes. The hydrogen bond pairs in these organic acid−ammonia complexes are classified as medium and weak.

Other structural modifications upon formation of the complexes involve the lengthening or shortening of the bonds adjacent to the hydrogen bonds (XO−H···Y) (X = S or C and Y = O or N) or (Z−H···O) (Z = N or O). For example, the O−H bond length in the *cis*-pinonic acid−sulfuric acid complex is increased by 0.02 and 0.06 Å for the weaker and the stronger hydrogen bond, respectively. Similarly, in the case of benzoic acid−ammonia complex, the O−H and N−H bonds are elongated by 0.04 and 0.01 Å, respectively. The lengthening or shortening of these bonds is a result of the balance between hyperconjugation and rehybridization, which act in the opposite directions in respect to the bond length. The hyperconjugative interaction (or charge transfer) from the lone pair of the hydrogen bond acceptor to the antibonding σ*(O−H or N−H) orbital of the hydrogen bond donor leads to the lengthening of the O−H or N−H bond. The increase in s-character of the O−H or N−H bond due to the decrease of the effective electronegativity of the hydrogen atom upon the formation of hydrogen bond results in the shortening of the N−H or O−H bond.[57] The calculated lengthening of the N−H or O−H bond is a result of the balance between these two effects, with the hyperconjugation dominant over the rehybridization for all hydrogen-bonded complexes studied here as confirmed by Natural Bonding Orbital (NBO) analysis.[54] While rehybridization of the O−H and N−H bonds upon the complex formation is insignificant, there is effective charge transfer (CT) from the lone pairs of oxygen and nitrogen to the antibonding orbital of the O−H. According to the second-order perturbation analysis, the CT interaction is about 60−70 kcal mol^{-1} for the short hydrogen bond and 20−30 kcal mol^{-1} for the long hydrogen bond. The domination of charge transfer resulting in the longer N−H and O−H bonds is also reflected in the charge distribution around the cyclic hydrogen bond ring structure. For example, the calculated Mulliken charges of the hydrogen atoms participating in the hydrogen bond pair are increased from 0.359 for sulfuric acid and 0.321 for *cis*-pinonic acid to 0.415 and 0.380 for the *cis*-pinonic acid−sulfuric acid complex, indicating a decrease in the effective electronegativity of hydrogen upon the hydrogen bond formation. Similar increases in the Mulliken charges of

TABLE 5: Thermochemical Parameters for the Complex Formation Calculated at G2(MP2, SVP) and CCSD(T)+CF Levels[a]

	G2(MP2, SVP)[b]				CCSD(T)+CF[c]			
complex	E_B	ΔH	ΔS	ΔG	E_B	ΔH	ΔS	ΔG
BA_SA	17.84	−18.30	−36.06	−7.55	17.62	−17.58	−37.03	−6.54
BA_AM	9.43	−10.41	−31.63	−0.98	9.27	−9.72	−30.78	−0.54
AA_AM	8.85	−8.99	−30.12	−0.01	8.45	−8.97	−30.75	0.20
FA_AM	9.18	−9.46	−30.12	−0.48	8.73	−9.38	−30.59	−0.26

[a] E_B (kcal mol^{-1}), ΔH (kcal mol^{-1}), ΔS (cal mol^{-1} K^{-1}), and ΔG (kcal mol^{-1}) are the changes in binding energy, enthalpy, entropy, and Gibbs free energy, respectively. Zero point energy, entropy, and thermal corrections to enthalpy and Gibbs free energy correspond to 1 atm, 298 K. [b] Vibrational analysis performed at the HF/6-31G(d) level of theory. [c] Vibrational analysis performed at the B3LYP/6-31G(d,p) level of theory.

the hydrogen atoms in other investigated hydrogen-bonded complexes are also observed.

Lengthening or shortening of the bonds in the monomer moieties results in the red or blue shift of the stretching frequencies upon the formation of the hydrogen bonds. Table 3 summarizes the shifts of the stretching frequencies for the formation of dimers between sulfuric acid, organic acid, ammonia, and/or water. For example, the lengthening of the SO−H and CO−H bonds in the *cis*-pinonic acid−sulfuric acid complex is 0.057 and 0.020 Å, respectively, resulting in red shifts of the corresponding stretching frequencies of 1066 and 391 cm^{-1} (unscaled). For the same complex, the S═O and C═O bond lengths are increased by 0.019 and 0.023 Å, respectively, corresponding to a red shift of 295 and 105 cm^{-1}. The only blue shift of −59 cm^{-1} in the *cis*-pinonic acid−sulfuric acid complex is ∼0.05 Å shortening of the S−OH bond. The absorption intensities of the monomers and the hydrogen-bonded complexes and the distinct features of the corresponding IR spectra are listed in Figure S1 (Supporting Information) for the PA-SA complex, in which the most intense absorption peaks are related to the vibrational stretching modes of the hydrogen bonds. It needs to be pointed out that increased anharmonicity due to hydrogen-bonding interactions may lead to underestimation of the calculated shifts in vibrational frequencies.

3.2. Thermochemical Analysis. Relevant thermochemical parameters (e.g., binding energy, enthalpy, entropy, and Gibbs free energy) for the complex formation at 1 atm and 298 K are calculated at several theoretical levels with different basis sets. The energy and other thermochemical data are taken from the Gaussian calculations and the thermochemical properties are computed from vibrational analysis by using unscaled frequencies,[60]

$$\Delta_r E_B^o(0\mathrm{K}) = \sum(\varepsilon_0 + \mathrm{ZPE})_{\mathrm{prod}} - \sum(\varepsilon_0 + \mathrm{ZPE})_{\mathrm{react}} \quad (1)$$

$$\Delta_r H^o(298\mathrm{K}) = \sum(\varepsilon_0 + H_{\mathrm{corr}})_{\mathrm{prod}} - \sum(\varepsilon_0 + H_{\mathrm{corr}})_{\mathrm{react}} \quad (2)$$

$$\Delta_r G^o(298\mathrm{K}) = \sum(\varepsilon_0 + G_{\mathrm{corr}})_{\mathrm{prod}} - \sum(\varepsilon_0 + G_{\mathrm{corr}})_{\mathrm{react}} \quad (3)$$

$$\Delta_r S^o(298\mathrm{K}) = \frac{\Delta_r H^o(298\mathrm{K}) - \Delta_r G^o(298\mathrm{K})}{298} \quad (4)$$

where$\Delta_r E_B^o(0\mathrm{K})$, $\Delta_r H^o(298\mathrm{K})$, $\Delta_r G^o(298\mathrm{K})$, and $\Delta_r S^o(298\mathrm{K})$are binding energy, enthalpy, Gibbs free energy, and entropy, respectively, and ε_0, ZPE, H_{corr}, and G_{corr} are the total energy at 0 K, zero-point energy correction, and thermal corrections to enthalpy and Gibbs free energy at 298 K, respectively. Tables 4−7 summarize the thermochemical parameters for complexes of sulfuric acid, organic acids, ammonia, and water computed at different levels of theory. The binding energies are strongly dependent on the selection of the method and basis set. As shown in Table 4, B3LYP/6-31G(d,p) predicts the highest binding energies, ranging from 9.5 to 16.3 kcal mol^{-1} for different complexes after correction for basis set superposition error (BSSE). The effect of BSSE estimated by using the counterpoise correction (CP) method is large and reaches 4.1 kcal mol^{-1} at the B3LYP/6-31G(d,p) level. Single-point energy calculations at the B3LYP/6-311++G(2d,2p) level for the B3LYP/6-31G(d,p)-optimized structures reduce the bonding energies of complexes by about 4 kcal mol^{-1}. Using a large 6-311++G(2d,2p) basis set also results in significantly lower BSSE in the range of 0.4−1.0 kcal mol^{-1}. Clearly, application of the counterpoise correction reduces the difference between the CP-corrected binding energies calculated by using different basis sets to below 1.4 kcal mol^{-1} (Table 4). This has an important implication for calculation of energetic properties of larger clusters containing tens or hundreds of molecules where the use of large basis sets may be computationally prohibitive.

The formation enthalpies for the sulfuric acid complexes with water (−8.3 kcal mol^{-1}) and ammonia (−12.9 kcal mol^{-1}) calculated by using the CP-corrected B3LYP/6-311++G(2d,2p) energies (Table 4) are within 0.7 and 0.3 kcal mol^{-1} of the values derived by Kurten et al.[22] at the same level of theory with the CP correction to both the energy and geometry and are also within 1.5 kcal mol^{-1} of the results of CP-corrected MP2 calculations.[22] However, discrepancies ranging from 3 to 6 kcal mol^{-1} are observed between our results and the results obtained with PW91 density functional.[22,30] For instance, at the PW91/6-311++G(3df,3pd) level of theory,[30] the formation enthalpies for the complexes of formic and acetic acid with ammonia were found to be −11.6 and −10.8 kcal mol^{-1} compared to the values of −8.7 and −7.8 kcal mol^{-1} calculated in our study (Table 4). A close agreement between the reaction energies produced by B3LYP and MP2 and a systematic difference between these two methods and PW91 has been reported recently.[22]

In addition to B3LYP calculations, we evaluated the stability of complexes using G2(MP2,SVP) and CCSD(T)+CF composite methods, which produce the total energies effectively corresponding to QCISD(T)/6-311+G(3df,2p) and CCSD(T)/6-311G++G(d,p) levels, respectively. As shown in Table 5, composite methods agree with each other within 0.5 kcal mol^{-1}, but the binding energies produced are 0.7 to 2.7 kcal mol^{-1} higher than those derived with CP-corrected B3LYP/6-311++G(2d,2p). It is well-known that the convergence in terms of the higher angular momentum functions (i.e., the size of basis set) is slower in correlated methods than in the HF and DFT calculations. Also, for methods including electron correlation, the CP correction is larger and more sensitive to the basis set size. For instance, a recent study of sulfuric acid complexes with ammonia and water has shown that for the same basis set counterpoise correction is smaller at the B3LYP level than at MP2 or CCSD(T) levels of theory.[22] To gain more information about the effect of basis set on BSSE in ab inito and DFT calculations of hydrogen-bonded complexes, we compute the change in electronic energy and the corresponding counterpoise correction for the formic acid−ammonia complex at CCSD(T) and B3LYP levels of theory with several different basis sets (Table 6). For both methods, the complex formation energy roughly converges with the 6-311++G(2d,p) basis set, but the counterpoise correction obtained at the CCSD(T) level (1.8 kcal mol^{-1}) remains higher than that calculated with B3LYP (0.6

TABLE 6: The Effect of the Basis Set on the Formation Energy and Counterpoise Correction for the Formic Acid−Ammonia Complex at B3LYP and CCSD(T) Theory Levels[a]

	CCSD(T)			B3LYP		
basis set	ε_0	E_{CP}	$\varepsilon_0 + \varepsilon_{CP}$	ε_0	E_{CP}	$\varepsilon_0 + \varepsilon_{CP}$
CCSD(T)/6-31G(d)	−14.21	4.09	−10.12	−15.59	2.78	−12.81
CCSD(T)/6-311G(d,p)	−13.50	5.09	−8.41	−14.82	3.96	−10.86
CCSD(T)/6-311++G(d,p)	−11.57	2.67	−8.90	−11.80	0.83	−10.97
CCSD(T)/6-311++G(2d,p)	−11.52	1.81	−9.72	−11.16	0.62	−10.55

[a] ε_0 and ε_{CP} are the change in the total electronic energy and the counterpoise correction for the complex formation, respectively; single point energies are computed for geometries optimized at the B3LYP/6-31G(d,p) level.

TABLE 7: Thermochemical Parameters for the Complex Formation Calculated at the B3LYP Level with Counterpoise Correction to the Energy[a]

	B3LYP/6-31G(d,p)					B3LYP/6-311++G(2d,2p)			
complex	E_{CP}	E_B	ΔH	ΔS	ΔG	E_{CP}	E_B	ΔH	ΔG
PA_SA_W	7.84	25.47	−26.25	−69.10	−5.64	1.81	21.52	−22.30	−1.69
PA_SA_SA	6.77	29.55	−29.56	−73.48	−7.65	2.30	26.34	−26.36	−4.45
PA_SA_PA	7.22	30.98	−30.87	−75.32	−8.42	1.07	29.18	−29.06	−6.61

[a] E_{CP} (kcal mol^{-1}) is the counterpoise correction; E_B (kcal mol^{-1}), ΔH (kcal mol^{-1}), ΔS (cal mol^{-1} K^{-1}), and ΔG (kcal mol^{-1}) are changes in binding energy, enthalpy, entropy, and Gibbs free energy, respectively. Zero point energy, entropy, and thermal corrections to enthalpy and Gibbs free energy were calculated from vibrational analysis performed at the B3LYP/6-31G(d,p) level of theory (1 atm, 298 K).

kcal mol^{-1}). The composite G2(MP2, SVP) and CCSD(T)+CF methods likely produce the most reliable binding energies.

The choice of method and basis set has a relatively small effect on entropy and the thermal corrections to enthalpy and Gibbs free energy of hydrogen-bonded complex formation.[22] Comparison of the data in Tables 4 and 5 shows that thermochemical analysis based on HF/6-31G(d) and B3LYP/6-31G(d,p) frequencies produces very similar complex formation entropies. Moreover, the entropy changes are practically independent of the nature of organic acid and only vary with the structure of the cyclic ring formed by a hydrogen bond pair, i.e., about −37 cal mol^{-1} K^{-1} for the acid−acid complexes and about −31 cal mol^{-1} K^{-1} for the acid−ammonia complexes.

As shown in Table 4, at the B3LYP/6-311++G(2d,2p) level of theory the strongest complexes are the homomolecular dimers formed from two organic acid molecules and the heteromolecular dimers of organic acids with sulfuric acid (formation enthalpies −13.2 to −14.9 kcal mol^{-1}), followed in an order of decreasing strength by sulfuric acid−ammonia complex (−12.9 kcal mol^{-1}) and sulfuric acid homomolecular dimer (−11.8 kcal mol^{-1}). Sulfuric acid monohydrate and complexes of organic acids and ammonia are the weakest and of comparable strengths (−8.0 to −8.3 kcal mol^{-1}). The higher binding energies for the organic acid−sulfuric acid and organic acid−organic acid complexes reflect stronger hydrogen bonding, consistent with the geometrical analysis.

Sulfuric acid has been commonly identified as a key species in new particle formation,[3,61] a process that involves collisions of sulfuric acid and water molecules to form clusters, some of which grow above the critical size of about 1 nm to eventually become nanoparticles. Low concentration of sulfuric acid in the troposphere ($\sim 10^5$ molecule cm^{-3} daytime average, rising to $\sim 10^7$ molecule cm^{-3} during nucleation events) limits the growth of clusters via sulfuric acid condensation and it is commonly recognized that binary nucleation is not efficient enough to explain observed nucleation events.[62] A laboratory study has shown that addition of 10^9 molecule cm^{-3} concentration of aromatic acids enhances the sulfuric acid−water vapor nucleation rate by more than an order of magnitude.[11] Hence, anthropogenic and biogenic carboxylic acids, present in the troposphere in concentrations ranging from 10^7 to 10^9 molecule cm^{-3}, potentially contribute to the nucleation process through either homomolecular complexes or complexes with sulfuric acid. Although homomolecular dimers of organic acids have strong binding energies (Table 4), no hydrogen acceptor or donor groups are available in these complexes for addition of water, sulfuric acid, or organic acid molecules to promote subsequent growth. Hence, homomolecular dimers are unlikely to contribute to new particle formation. In the heteromolecular complexes between sulfuric acid and organic acids, a vacant OH group remains available in the sulfuric acid moiety to support further growth of the complex through the formation of strong hydrogen bonds (Figure 1). Also, addition of a third molecule to the *cis*-pinonic acid−sulfuric acid complex results in further stabilization by −7.3, −12.1, and −14.9 kcal mol^{-1} for water, sulfuric acid, and organic acid (Table 7).

TABLE 8: Equilibrium Constants (K) of Sulfuric Acid Complexes[a]

complex	K, cm^3 molecule^{-1}
SA-SA	2.3×10^{-19}
SA-PA	5.9×10^{-18}
SA-BA	2.7×10^{-17}
SA-AM	2.9×10^{-17}
SA-W	5.2×10^{-21}

[a] Determined by using the results at the B3LYP/6-31G(d,p) level of theory.

Formation of organic acid−sulfuric acid complexes corresponds to the Gibbs free energy changes of −3.8 kcal mol^{-1} for benzoic acid and −2.9 kcal mol^{-1} for *cis*-pinonic acid. Upon addition of sulfuric acid or *cis*-pinonic acid, these bimolecular complexes are further stabilized by −2.8 to −3.8 kcal mol^{-1}. Table 8 shows a comparison of the equilibrium constants for the various sulfuric acid complexes determined at the B3LYP/6-311++G(2d,2p) level of theory. It should be pointed out that the concentrations of dimers and trimers during the nucleation process in the atmosphere cannot be directly calculated from the equilibrium constants, since equilibrium is hardly established due to very low atmospheric concentrations of the nucleation precursors. Instead, an explicit kinetic mechanism of the complex formation, decomposition, and growth to larger size must be considered to determine the abundances of the

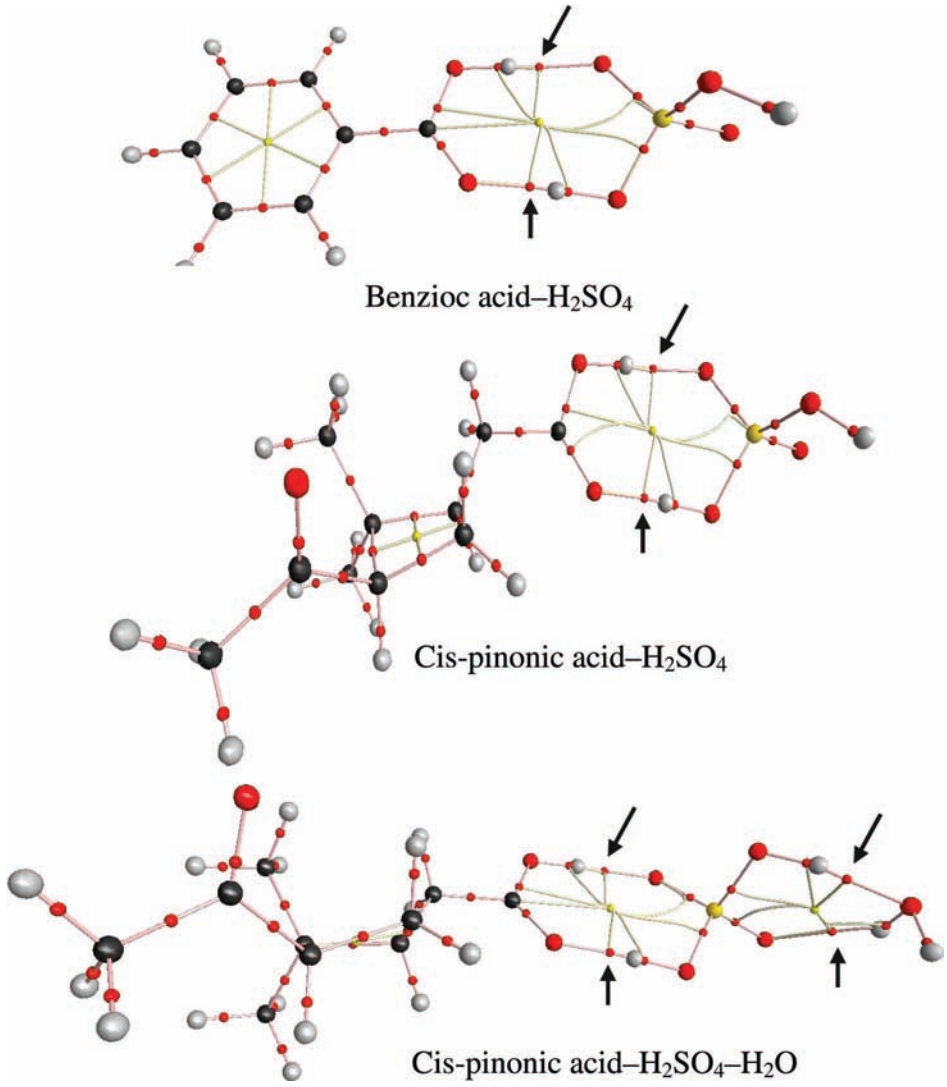

Figure 3. Molecular graphs of the organic acid−sulfuric acid complexes showing the BCPs, ring critical points, bond path, and ring path.

complexes by solving time-dependent differential equations. If the growth process is fast, a complex can still be an important intermediate on the reaction path toward formation of stable clusters even though its steady-state concentration is low. Organic acids, because of their relatively large molecular size (∼1 nm) and strong hydrogen bonding with sulfuric acid, can greatly assist the growing clusters in overcoming the critical size and hence increase the nucleation rate. Further insight into the effect of organic acids on nucleation can be gained by studying the distributions of clusters of different composition involving sulfuric acid, organic acid, and water molecules.[25,63]

3.3. Topological Analysis. Topological properties of the hydrogen bonds provide alternative ways to study the hydrogen bond strength. According to Bader's theory of atoms in molecules,[36] the nuclei are defined as the attractors of the gradient vector field of charge distribution, which are denoted as (3, −3) critical points and have maxima of charge density. An atom is thus viewed as the union of an attractor (nucleus) and its associated basin (electron density distribution). The bond critical point (BCP) is defined as the point at which the Hessian matrix of the charge density has two negative and one positive eigenvalues. The bond path is the line formed from two paths, both of which originate from the bond critical points and terminate at neighboring attractors. The bond critical points of the electron densities of the complexes and clusters are calculated and identified in the molecular graphs (Figures 3 and 4). A notable topological feature of the complexes is that there exists a nearly planar, 6- or 8-membered cyclic ring structure with a pair of hydrogen bonds and for each hydrogen bond, the BCP lies close to the H nuclei, consistent with the topological structures of $H_2SO_4-H_2O$ and $H_2SO_4-NH_3$ by Kurten et al.[22] Topological parameters (e.g., charge density and its Laplacian, the electronic kinetic, potential, and total energies) at the bond critical points (BCPs) can be employed to evaluate the nature of hydrogen-bonding interactions in the complexes. Koch and Popelier proposed eight topological criteria based on the theory of atoms in molecules to characterize the types of hydrogen bonds.[64] The closed-shell interactions (e.g., ionic bonds, hydrogen bonds, and van der Waals interactions) correspond to a positive value of Laplacian of charge density at BCP, whereas for covalent bonds the Laplacian has a negative value. The strength of the hydrogen bonds correlates with the charge density and, in general, the larger the charge density, the stronger the hydrogen bond. Two quantitative criteria have been suggested to characterize the strength of a hydrogen bond: the charge density and its Laplacian, in the range of 0.002−0.035 and 0.024−0.139 au, respectively.[56] As shown in Table 9, the value of charge density of the stronger hydrogen bond of the pair in this study ranges from 0.046 to 0.080 au and these values exceed the upper value of charge density proposed by Koch and

TABLE 9: Topological Parameters (Charge Densities, Laplacian, Kinetic Energy Densities, Potential Energy Densities, and Total Energy Densities) at BCPs of the Hydrogen Bonds of the Complexes (in au)[a]

complex	ρ (10^{-2})	∇^2 (10^{-2})	G(r) (10^{-2})	V(r) (10^{-2})	K(r) (10^{-2})	ρ (10^{-2})	$\nabla^2\rho$ (10^{-2})	G(r) (10^{-2})	V(r) (10^{-2})	K(r) (10^{-2})
			hydrogen bond 1					hydrogen bond 2		
SA-W a	5.53	14.44	4.02	−4.43	−0.41	2.02	6.37	1.63	−1.66	−0.03
b	4.64	12.11	3.49	−3.95	−0.46	1.48	5.43	1.20	−1.04	0.16
SA-AM	7.96	8.88	4.65	−7.08	−2.43	1.24	4.46	1.02	−0.93	0.09
SA-SA	4.58	14.07	3.51	−3.50	0.01					
BA-BA	5.42	14.77	3.98	−4.28	−0.29					
PA-PA	5.11	14.16	3.73	−3.93	−0.19					
BA-SA	7.20	15.61	5.31	−6.72	−1.41	4.09	12.64	3.10	−3.04	0.06
PA-SA	6.87	15.71	5.07	−6.21	−1.14	3.96	12.19	2.98	−2.92	0.06
AA-AM	5.13	10.72	3.20	−3.71	−0.52	1.67	5.20	1.29	−1.28	0.01
BA-AM	5.38	10.95	3.35	−3.96	−0.61	1.61	5.12	1.26	−1.23	0.02
FA-AM	5.44	10.89	3.37	−4.01	−0.65	1.46	4.75	1.14	−1.10	0.04
PA-SA-W	6.49	15.73	4.80	−5.67	−0.87	4.08	12.52	3.08	−3.02	0.05
PA-SA-SA	7.35	15.36	5.38	−6.93	−1.54	3.87	11.91	2.91	−2.85	0.06
PA-SA-PA	6.63	15.66	4.88	−5.85	−0.97	4.03	12.37	3.04	−2.99	0.05
			hydrogen bond 3					hydrogen bond 4		
PA-SA-W	5.35	14.14	3.89	−4.24	−0.35	2.04	6.35	1.63	−1.67	−0.04
PA-SA-SA	4.87	14.60	3.72	−3.80	−0.08	4.47	13.72	3.41	−3.40	0.02
PA-SA-PA	6.60	15.73	4.87	−5.81	−0.94	4.04	12.37	3.04	−2.99	0.05

[a] Geometries of the complexes are optimized at B3LYP/6-31G(d,p) except for SA-W (b), which was optimized at B3LYP/6-311++g(2d,2p).

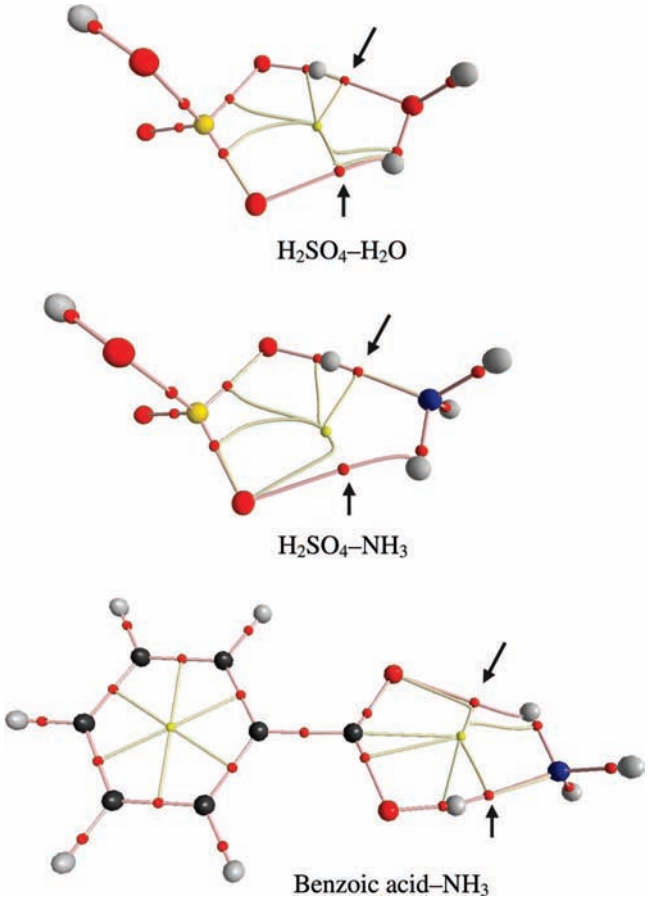

Figure 4. Molecular graphs of the sulfuric acid−water, sulfuric acid−ammonia, and benzoic acid−ammonia complexes showing the BCPs, ring critical points, bond path, and ring path.

Popelier.[61] The values of the charge density and its Laplacian of H_2SO_4−H_2O and H_2SO_4−NH_3 are in good agreement with those by Kurten et al., while the values of the total energy density are two order magnitudes lower than those previously reported.[22] Similarly, the Laplacian of charge density of the complexes composed of sulfuric acid, organic acid, and water is in the range of 0.14−0.16 au, higher than the upper value of the Laplcian criteria. The high values of the charge density and Laplican indicate that the hydrogen-bonding interaction between sulfuric acid and organic acids is quite strong, consistent with the given above geometrical characterization as approaching the covalent bonding for the stronger hydrogen bond of the pair. For the organic acid−sulfuric acid complexes, the weaker hydrogen bond of the pair is classified as medium strength as mentioned in the geometrical analysis, which is seen (Table 9) from the values of the charge density and the Laplacian, in the range of 0.039−0.045 and 0.12−0.14 au, respectively. However, for sulfuric acid monohydrate and ammonia−sulfuric acid (or organic acids) complexes, the hydrogen bond pair is only of medium-to-low strength according to generally lower values of both charge density and Laplacian of these hydrogen bonds at BCPs, which is also consistent the geometrical analysis.

The electronic energy density $K(r)$ can also be used to characterize the bonding strength of the hydrogen bonds, and $K(r)$ is related to the Laplacian of the charge density by a local expression of the virial theorem,[36]

$$\left(\frac{\hbar}{4m}\right)\nabla^2\rho(r) = K(r) + G(r) \tag{5}$$

where $K(r) = G(r) + V(r)$, $G(r)$ is the electronic kinetic energy density, which is always positive, and $V(r)$ is the electronic potential energy density, which is always negative. m and $\hbar$ are the mass of an electron and the Planck constant, respectively. A positive Laplacian at a BCP indicates that the hydrogen-bonding interaction is dominated by the contraction of the charge away from the interatomic surface toward each nucleus and depletion of the charge along the bond path. For the hydrogen-bonding interactions in this study, the Laplacian is found to be positive, indicating that the electronic kinetic energy density is in local excess over the magnitude of the corresponding total electronic energy density in the virial theorem, $G(r) > K(r)$ (or $2G(r) > V(r)$). In addition, for strong hydrogen-bonding interaction, the total electronic energy density $K(r)$ is found to be negative (Table 9), showing partially covalent and partially electrostatic in nature, whereas this quantity is positive for medium and weak hydrogen bonds, revealing only electrostatic interactions for this bonding.

4. Conclusions

Formation of molecular complexes and clusters from potential atmospheric aerosol nucleation precursors has been investigated by theoretical methods by using quantum chemical calculations to explore the structures, energetics, and topology of complexes composed of sulfuric acid, organic acid, ammonia, and water. Geometrical analysis shows that organic acid−sulfuric acid complexes bear a pair of hydrogen bonds with one strong and one medium-strength hydrogen bonding, while for organic acid−ammonia complexes the corresponding hydrogen bond pair is much weaker. The binding energies for organic acid−sulfuric acid complexes are also higher than those for organic acid−ammonia complexes by several kcal mol^{-1}. Topological analysis employing quantum theory of atoms in molecules (QTAIM) shows that the charge density and the Laplacian at BCPs of the hydrogen bonds of the organic acid−sulfuric acid are positive and fall in the range or exceed the range of one strong and one medium-strength hydrogen bonding criteria. In the atmosphere, due to the abundance of the organic acids, strong hydrogen-bonding interactions between organic acid and sulfuric acid provide a driving force for the formation of organic acid−sulfuric acid complex, which is likely responsible for a reduction of nucleation barrier by modifying the hydrophobic properties of organic acid and allowing further addition of hydrophilic species (e.g., H_2SO_4, H_2O, and possibly NH_3) to the hydrophilic side of the clusters, propelling the nascent growth of the new particles. This study provides the geometrical, energetical, and topological information of hydrogen-bonding interactions in the atmospheric complexes and helps to elucidate the structure, size, composition, and other properties of atmospheric clusters, bridging the gap between the molecule and the newly formed nuclei.

Acknowledgment. This work was supported by the Robert A. Welch Foundation (Grant A-1417). Additional support was provided by the Texas A&M University Supercomputing Facilities. The authors acknowledged the use of the Laboratory for Molecular Simulations at Texas A&M and Dr. Lisa M. Pérez for assistance with the calculations. Two referees provided helpful suggestions to improve this paper. R.Z. acknowledged additional support from National Natural Science Foundation of China Grant (40728006). Work at the BNL was supported under the DOE Atmospheric Sciences Program.

Supporting Information Available: Tables giving a comparison of sulfuric acid bond lengths and angles with literature data, a comparison of water and ammonia bond lengths and angles with leterature data, a comparison of organic acids bond lengths and angles with literature data, and Cartesian coordinated and absolute energies of monomers and complexes optimized at the B3LYP/6-31G(d,p) level, as well as a figure of the calculated infrared spectra of the *cis*-pinonic acid−sulfuric acid complex and its monomers. This material is available free of charge via the Internet at http://pubs.acs.org.

References and Notes

(1) Kanakidou, M.; Seinfeld, J. H.; Pandis, S. N.; Barnes, I.; Dentener, F. J.; Facchini, M. C.; Van Dingenen, R.; Ervens, B.; Nenes, A.; Nielsen, C. J.; Swietlicki, E.; Putaud, J. P.; Balkanski, Y.; Fuzzi, S.; Horth, J.; Moortgat, G. K.; Winterhalter, R.; Myhre, C. E. L.; Tsigaridis, K.; Vignati, E.; Stephanou, E. G.; Wilson, J. *Atmos. Chem. Phys.* **2005**, *5*, 1053.

(2) Kulmala, M.; Vehkamaki, H.; Petajda, T.; Dal Maso, M.; Lauri, A.; Kerminen, V. M.; Birmili, W.; McMurry, P. H. *J. Aerosol Sci.* **2004**, *35*, 143.

(3) McMurry, P. H.; Fink, M.; Sakurai, H.; Stolzenburg, M. R.; Mauldin, R. L.; Smith, J.; Eisele, F.; Moore, K.; Sjostedt, S.; Tanner, D.; Huey, L. G.; Nowak, J. B.; Edgerton, E.; Voisin, D. *J. Geophys. Res.* **2005**, *110*, D22S02, doi 10.1029/2005JD005901.

(4) Kim, T. O.; Ishida, T.; Adachi, M.; Okuyama, K.; Seinfeld, J. H. *Aerosol Sci. Technol.* **1998**, *29*, 111.

(5) Ball, S. M.; Hanson, D. R.; Eisele, F. L.; McMurry, P. H. *J. Geophys. Res., Atmos.* **1999**, *104*, 23709.

(6) Coffman, D. J.; Hegg, D. A. *J. Geophys. Res., Atmos.* **1995**, *100*, 7147.

(7) Korhonen, P.; Kulmala, M.; Laaksonen, A.; Viisanen, Y.; McGraw, R.; Seinfeld, J. H. *J. Geophys. Res., Atmos.* **1999**, *104*, 26349.

(8) Napari, I.; Kulmala, M.; Vehkamaki, H. *J. Chem. Phys.* **2002**, *117*, 8418.

(9) Napari, I.; Noppel, M.; Vehkamaki, H.; Kulmala, M. *J. Chem. Phys.* **2002**, *116*, 4221.

(10) Hanson, D. R.; Eisele, F. L. *J. Geophys. Res., Atmos.* **2002**, 107.

(11) Zhang, R. Y.; Suh, I.; Zhao, J.; Zhang, D.; Fortner, E. C.; Tie, X. X.; Molina, L. T.; Molina, M. J. *Science* **2004**, *304*, 1487.

(12) Zhang, R.; Wooldridge, P. J.; Abbatt, J. P. D.; Molina, M. J. *J. Phys. Chem.* **1993**, *97*, 7351.

(13) Zhang, R.; Wooldridge, P. J.; Molina, M. J. *J. Phys. Chem.* **1993**, *97*, 8541.

(14) Kurdi, L.; Kochanski, E. *Chem. Phys. Lett.* **1989**, *158*, 111.

(15) Arstila, H.; Laasonen, K.; Laaksonen, A. *J. Chem. Phys.* **1998**, *108*, 1031.

(16) Bandy, A. R.; Ianni, J. C. *J. Phys. Chem. A* **1998**, *102*, 6533.

(17) Re, S.; Osamura, Y.; Morokuma, K. *J. Phys. Chem. A* **1999**, *103*, 3535.

(18) Ding, C. G.; Laasonen, K.; Laaksonen, A. *J. Phys. Chem. A* **2003**, *107*, 8648.

(19) Ding, C. G.; Laasonen, K. *Chem. Phys. Lett.* **2004**, *390*, 307.

(20) Ianni, J. C.; Bandy, A. R. *J. Mol. Struct.: THEOCHEM* **2000**, *497*, 19.

(21) Al Natsheh, A.; Nadykto, A. B.; Mikkelsen, K. V.; Yu, F. Q.; Ruuskanen, J. *J. Phys. Chem. A* **2004**, *108*, 8914.

(22) Kurten, T.; Sundberg, M. R.; Vehkamaki, H.; Noppel, M.; Blomqvist, J.; Kulmala, M. *J. Phys. Chem. A* **2006**, *110*, 7178.

(23) Ianni, J. C.; Bandy, A. R. *J. Phys. Chem. A* **1999**, *103*, 2801.

(24) Larson, L. J.; Largent, A.; Tao, F. M. *J. Phys. Chem. A* **1999**, *103*, 6786.

(25) Kurten, T.; Torpo, L.; Ding, C. G.; Vehkamaki, H.; Sundberg, M. R.; Laasonen, K.; Kulmala, M. *J. Geophys. Res., Atmos.* **2007**, *112*, D04210, doi 10.1029/2006JD007391.

(26) Emmeluth, C.; Suhm, M. A. *Phys. Chem. Chem. Phys.* **2003**, *5*, 3094.

(27) Nandi, C. K.; Hazra, M. K.; Chakraborty, T. *J. Chem. Phys.* **2005**, 123.

(28) Sloth, M.; Bilde, M.; Mikkelsen, K. V. *Mol. Phys.* **2004**, *102*, 2361.

(29) Gora, R. W.; Grabowski, S. J.; Leszczynski, J. *J. Phys. Chem. A* **2005**, *109*, 6397.

(30) Nadykto, A. B.; Yu, F. Q. *Chem. Phys. Lett.* **2007**, *435*, 14.

(31) Koch, S.; Winterhalter, R.; Uherek, E.; Kolloff, A.; Neeb, P.; Moortgat, G. K. *Atmos. Environ.* **2000**, *34*, 4031.

(32) Capouet, M.; Muller, J. F. *Atmos. Chem. Phys.* **2006**, *6*, 1455.

(33) Fan, J.; Zhang, R.; Collins, D.; Li, G. *Geophys. Res. Lett.* **2006**, *33*, L15802, doi 10.1029/2006GL026295.

(34) McGraw, R.; Zhang, R. *J. Chem. Phys.* **2008**, *128*, 064508, doi 10.1063/1.2830030.

(35) Kavouras, I. G.; Mihalopoulos, N.; Stephanou, E. G. *Nature* **1998**, *395*, 683.

(36) Bader, R. F. W. *Atoms in molecules: a quantum theory*; Clarendon Press: Oxford; New York, 1990.

(37) Frisch, M. J.; Trucks, G. W.; Schlegel, H. B.; Scuseria, G. E.; Robb, M. A.; Cheeseman, J. R.; Montgomery, J. A., Jr.; Vreven, T.; Kudin, K. N.; Burant, J. C.; Millam, J. M.; Iyengar, S. S.; Tomasi, J.; Barone, V.; Mennucci, B.; Cossi, M.; Scalmani, G.; Rega, N.; Petersson, G. A.; Nakatsuji, H.; Hada, M.; Ehara, M.; Toyota, K.; Fukuda, R.; Hasegawa, J.; Ishida, M.; Nakajima, T.; Honda, Y.; Kitao, O.; Nakai, H.; Klene, M.; Li, X.; Knox, J. E.; Hratchian, H. P.; Cross, J. B.; Adamo, C.; Jaramillo, J.; Gomperts, R.; Stratmann, R. E.; Yazyev, O.; Austin, A. J.; Cammi, R.; Pomelli, C.; Ochterski, J. W.; Ayala, P. Y.; Morokuma, K.; Voth, G. A.; Salvador, P.; Dannenberg, J. J.; Zakrzewski, V. G.; Dapprich, S.; Daniels, A. D.; Strain, M. C.; Farkas, O.; Malick, D. K.; Rabuck, A. D.; Raghavachari, K.; Foresman, J. B.; Ortiz, J. V.; Cui, Q.; Baboul, A. G.; Clifford, S.; Cioslowski, J.; Stefanov, B. B.; Liu, G.; Liashenko, A.; Piskorz, P.; Komaromi, I.; Martin, R. L.; Fox, D. J.; Keith, T.; Al-Laham, M. A.; Peng, C. Y.; Nanayakkara, A.; Challacombe, M.; Gill, P. M. W.; Johnson, B.; Chen, W.; Wong, M. W.; Gonzalez, C.; Pople, J. A. *Gaussian 03*, Revision B.05; Gaussian, Inc.: Pittsburgh, PA, 2003.

(38) Smith, B. J.; Radom, L. *J. Phys. Chem.* **1995**, *99*, 6468.

(39) Lei, W. F.; Derecskei-Kovacs, A.; Zhang, R. Y. *J. Chem. Phys.* **2000**, *113*, 5354.

(40) Lei, W. F.; Zhang, R. Y. *J. Chem. Phys.* **2000**, *113*, 153.

(41) Suh, I.; Lei, W. F.; Zhang, R. Y. *J. Phys. Chem. A* **2001**, *105*, 6471.
(42) Suh, I.; Zhang, D.; Zhang, R. Y.; Molina, L. T.; Molina, M. J. *Chem. Phys. Lett.* **2002**, *364*, 454.
(43) Zhang, D.; Zhang, R.; Park, J.; North, S. W. *J. Am. Chem. Soc.* **2002**, *124*, 9600.
(44) Suh, I.; Zhang, R. Y.; Molina, L. T.; Molina, M. J. *J. Am. Chem. Soc.* **2003**, *125*, 12655.
(45) Zhao, J.; Zhang, R.; Fortner, E. C.; North, S. W. *J. Am. Chem. Soc.* **2004**, *126*, 2686.
(46) Suh, I.; Zhao, J.; Zhang, R. Y. *Chem. Phys. Lett.* **2006**, *432*, 313.
(47) Lei, W.; Zhang, R.; McGivern, W. S.; Derecskei-Kovacs, A.; North, S. W. *Chem. Phys. Lett.* **2000**, *326*, 109.
(48) Zhang, D.; Lei, W.; Zhang, R. *Chem. Phys. Lett.* **2002**, *358*, 171.
(49) Biegler-Konig, F. *J. Comput. Chem.* **2000**, *21*, 1040.
(50) Biegler-Konig, F.; Schonbohm, J.; Bayles, D. *J. Comput. Chem.* **2001**, *22*, 545.
(51) Biegler-Konig, F.; Schonbohm, J. *J. Comput. Chem.* **2002**, *23*, 1489.
(52) Fiacco, D. L.; Hunt, S. W.; Leopold, K. R. *J. Am. Chem. Soc.* **2002**, *124*, 4504.
(53) Kollman, P. A.; Allen, L. C. *Chem. Rev.* **1972**, *72*, 283.
(54) Reed, A. E.; Curtiss, L. A.; Weinhold, F. *Chem. Rev.* **1988**, *88*, 899.
(55) Curtiss, L. A.; Blander, M. *Chem. Rev.* **1988**, *88*, 827.
(56) Gilli, P.; Bertolasi, V.; Ferretti, V.; Gilli, G. *J. Am. Chem. Soc.* **1994**, *116*, 909.
(57) Alabugin, I. V.; Manoharan, M.; Peabody, S.; Weinhold, F. *J. Am. Chem. Soc.* **2003**, *125*, 5973.
(58) Gilli, P.; Bertolasi, V.; Pretto, L.; Gilli, G. *J. Mol. Struct.* **2006**, *790*, 40.
(59) Pakiari, A. H.; Eskandari, K. *J. Mol. Struct.: THEOCHEM* **2006**, *759*, 51.
(60) Ochterski, J. W. *Thermochemistry in Gaussian*; Gaussian Inc.: Wallingford, CT, 2000.
(61) Weber, R. J.; McMurry, P. H.; Mauldin, R. L.; Tanner, D. J.; Eisele, F. L.; Clarke, A. D.; Kapustin, V. N. *Geophys. Res. Lett.* **1999**, *26*, 307.
(62) Boy, M.; Rannik, U.; Lehtinen, K. E. J.; Tarvainen, V.; Hakola, H.; Kulmala, M. *J. Geophys. Res.* **2003**, *108*, 4667.
(63) Kurten, T.; Torpo, L.; Sundberg, M. R.; Kerminen, V.-M.; Vehkamaki, H.; Kulmala, M. *Atmos. Chem. Phys.* **2007**, *7*, 2765.
(64) Koch, U.; Popelier, P. L. A. *J. Phys. Chem.* **1995**, *99*, 9747.

JP806693R